

# Phosphorylation-dependent Conformational Switch in Spin-labeled Phospholamban Bound to SERCA

Christine B. Karim\*, Zhiwen Zhang, Edmund C. Howard  
Kurt D. Torgersen and David D. Thomas

Department of Biochemistry  
Molecular Biology and  
Biophysics, University of  
Minnesota, Minneapolis, MN  
55455, USA

We have used chemical synthesis, functional reconstitution, and electron paramagnetic resonance (EPR) to probe the functional dynamics of phospholamban (PLB), which regulates the Ca-ATPase (SERCA) in cardiac sarcoplasmic reticulum. The transmembrane domain of PLB inhibits SERCA at low  $[Ca^{2+}]$ , but the cytoplasmic domain relieves this inhibition upon Ser16 phosphorylation. Monomeric PLB was synthesized with Ala11 replaced by the 2,2,6,6-tetramethylpiperidine-1-oxyl-4-amino-4-carboxylic acid (TOAC) spin label, which reports peptide backbone dynamics directly. PLB was reconstituted into membranes in the presence or absence of SERCA. TOAC-PLB showed normal inhibitory function, which was reversed by phosphorylation at Ser16 or by micromolar  $[Ca^{2+}]$ . EPR showed that the PLB cytoplasmic domain exhibits two resolved conformations, a tense *T* state that is ordered and a relaxed *R* state that is dynamically disordered and extended. PLB phosphorylation shifts this equilibrium toward the *R* state and makes it more dynamic (hyperextended). Phosphorylation strongly perturbs the dynamics of SERCA-bound PLB without dissociating the complex, while micromolar  $[Ca^{2+}]$  has no effect on PLB dynamics. A lipid anchor synthetically attached to the N terminus of PLB permits Ca-dependent SERCA inhibition but prevents the phosphorylation-induced disordering and reversal of inhibition. We conclude that the relief of SERCA inhibition by PLB phosphorylation is due to an order-to-disorder transition in the cytoplasmic domain of PLB, which allows this domain to extend above the membrane surface and induce a structural change in the cytoplasmic domain of SERCA. This mechanism is distinct from the one that relieves PLB-dependent SERCA inhibition upon the addition of micromolar  $[Ca^{2+}]$ .

© 2006 Elsevier Ltd. All rights reserved.

\*Corresponding author

Keywords: Ca-ATPase; cardiac; EPR; calcium transport; regulation

## Introduction

Phospholamban (PLB)<sup>1</sup> is a 52 residue integral membrane protein that regulates the enzymatic activity of sarco-endoplasmic reticulum Ca-ATPase (SERCA) in cardiac sarcoplasmic reticulum (SR).<sup>1</sup> The SERCA-PLB calcium-regulatory system has been implicated in cardiovascular disease.<sup>2–7</sup> Clarification of the physical mechanism by which

PLB regulates SERCA is needed to develop strategies for rescuing the failing heart muscle.

## Relief of inhibition does not require PLB dissociation from SERCA

It has been suggested that relief of inhibition, due to phosphorylation of PLB, micromolar  $[Ca^{2+}]$ , or mutation, is due to dissociation of PLB from SERCA, in a dynamic binding equilibrium, which also involves oligomeric interactions within PLB and within SERCA.<sup>2,8–13</sup> However, fluorescence resonance energy transfer (FRET) in functionally reconstituted membranes has shown that PLB binds tightly to SERCA in both the presence and absence of micromolar  $[Ca^{2+}]$ , so Ca-dependent relief of inhibition must be due to structural rearrangement

Abbreviations used: EPR, electron paramagnetic resonance; PLB, phospholamban; SERCA, sarco-endoplasmic reticulum Ca-ATPase; TOAC, 2,2,6,6-tetramethylpiperidine-1-oxyl-4-amino-4-carboxylic acid; WT, wild-type; DPC, dodecylphosphocholine.

E-mail address of the corresponding author:  
cbk@ddt.biochem.umn.edu

within the SERCA–PLB complex.<sup>12</sup> Similarly, other spectroscopic studies suggest that phosphorylation of PLB does not dissociate PLB from SERCA.<sup>14–17</sup> Thus, in the present study, we focus our attention on changes in the structure of the SERCA–PLB complex that occur with relief of inhibition due to phosphorylation of PLB or  $\text{Ca}^{2+}$  binding to SERCA.

### Structural dynamics of PLB in micelles and lipids

PLB is predominantly a homopentamer in membranes, with a small fraction of monomer,<sup>11,18</sup> but it has been shown by electron paramagnetic resonance (EPR),<sup>8,11</sup> fluorescence,<sup>19</sup> and mutagenesis<sup>10,18,20</sup> that the less predominant monomeric form of PLB is primarily responsible for inhibition of SERCA. Therefore, as in our previous studies, we focus on a stable and fully functional PLB monomer, designated AFA-PLB, obtained by replacing the three Cys residues (36, 41, and 46) to Ala, Phe, and Ala, respectively.<sup>21</sup> A high-resolution structural model of AFA-PLB has been obtained by NMR in detergent micelles,<sup>22</sup> and its orientation in lipid bilayers has been determined by solid-state NMR<sup>23</sup> and EPR.<sup>24,25</sup> The result is a model in which two helical domains are connected by a five-residue (17–21) semi-flexible loop in an L-shaped configuration (Figure 1, *T*). NMR relaxation studies showed that the PLB backbone structure in detergent micelles is actually quite dynamic throughout the cytoplasmic domain, especially in the region near the hinge-like loop.<sup>26</sup>

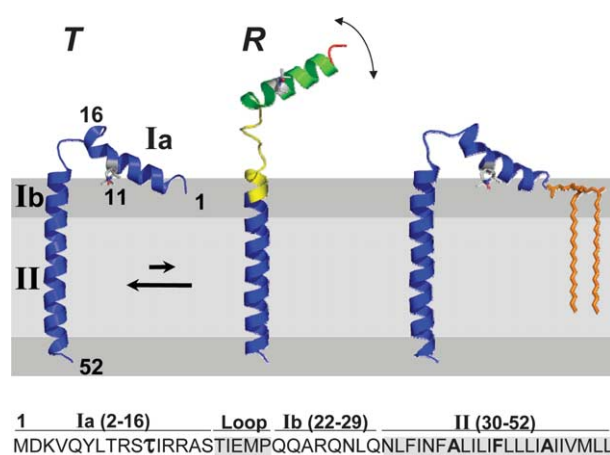


**Figure 1.** Two-state model for PLB structural dynamics in lipid bilayers, based on EPR of TOAC spin-labeled PLB.<sup>25</sup> Bottom: sequence of AFA-PLB with TOAC ( $\tau$ ) substituted for Ala at position 11. Left: cytoplasmic domain undergoes a dynamic equilibrium between *T* and *R* states. Right: a lipid anchor attached to the N terminus stabilizes only the *T* state. The *T* state is depicted as the average NMR solution structure,<sup>22</sup> while the *R* state (colored spectrally to indicate backbone dynamics increasing from blue to yellow to green to red<sup>25</sup>) is depicted as one of the more extended conformations from the ensemble of structures in that same NMR study.

### TOAC spin label

In order to elucidate PLB structural dynamics with high resolution in lipid bilayers, we previously synthesized monomeric AFA-PLB with the spin label 2,2,6,6-tetramethylpiperidine-1-oxyl-4-amino-4-carboxylic acid (TOAC) rigidly coupled to the  $\alpha$ -carbon, which thus reports directly the nanosecond rotational dynamics of the peptide backbone at the labeled site.<sup>25</sup> A probe in the transmembrane domain showed little nanosecond motion, indicating a stable  $\alpha$ -helix in this region, whereas three probes in different parts of the cytoplasmic domain all exhibited clearly a dynamic equilibrium between two conformational states, a predominant one (*T*, tense) that is helically ordered, and a minor population (*R*, relaxed) that is dynamically disordered on the nanosecond time scale, and is probably extended. The *T* and *R* nomenclature is used to discuss the cooperative allosteric interactions with SERCA that perturb the equilibrium between these two states.<sup>27</sup> We showed that the ordered conformation is stabilized by interaction with the membrane surface (Figure 1, *T*), whereas the dynamically disordered (extended) form (Figure 1, *R*) is poised to interact with SERCA, shifting the cytoplasmic domain above the membrane surface.<sup>24</sup> Both EPR and NMR studies in detergent micelles, and EPR in lipid bilayers, indicate that SERCA binds preferentially to the *R* conformation, consistent with an allosteric regulation mechanism.<sup>27</sup> NMR relaxation studies in micelles show that this conformational switch is affected by phosphorylation, which induces a further disorder-to-order transition.<sup>26</sup>

Here, we use TOAC-spin-labeled PLB to determine the changes in PLB structural dynamics in its regulatory complex with SERCA in lipid bilayers, when inhibition is relieved by  $\text{Ca}^{2+}$  binding to SERCA or phosphorylation of PLB. The effects of phosphorylation on these EPR spectra, in the presence and absence of SERCA, reveal new details about the role of structural dynamics in PLB regulation of SERCA. The effect of a lipid anchor attached to the N terminus of the cytoplasmic domain provides new insight into the importance of the cytoplasmic domain for the reversal of inhibition by phosphorylation.

## Results

### Secondary structure

Circular dichroism (CD) spectra (Figure 2) show that both AFA-PLB and its phosphoserine 16 derivative (Ser(P)16-AFA-PLB) are 85–90%  $\alpha$ -helical in lipid bilayers under EPR conditions, with a negligible change in helicity due to phosphorylation ( $-3(\pm 5)\%$ ). Similarly, phosphorylation had a negligible effect on the CD spectrum (not shown) under NMR conditions<sup>26</sup> (phosphate-buffered saline (pH 6.0), containing 300 mM DPC, at 37 °C).

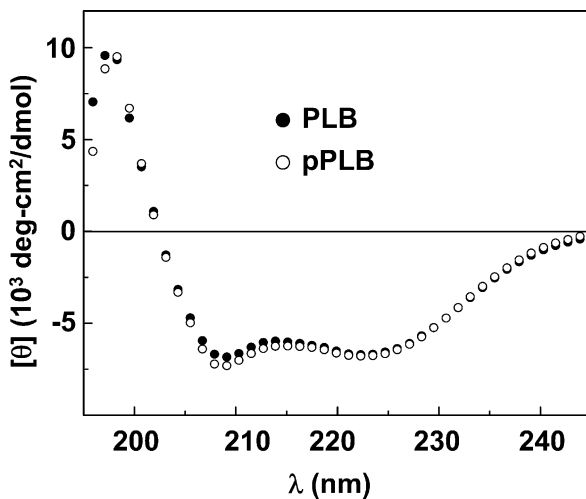


**Figure 2.** CD spectra of AFA-PLB, and its phosphorylated derivatives, in DOPC/DOPE bilayers (50:1, lipid/peptide) 10 mM Tris (pH 7.0). CD spectra were recorded on a Jasco J-710 spectrophotometer at 25 °C and analyzed as reported.<sup>21</sup> Spectra are plotted as mean residue ellipticity,  $[\theta]$ .

### Phosphorylation of Ser16 relieves SERCA inhibition

The inhibition of Ca-ATPase activity was quantified by the shift in  $pK_{Ca}$  (the pCa value required for 50% activation). We showed previously that AFA-PLB has similar inhibitory activity as wild-type (WT)-PLB, and that AFA-PLB retains inhibitory potency when Ala11 is replaced by TOAC.<sup>25</sup>

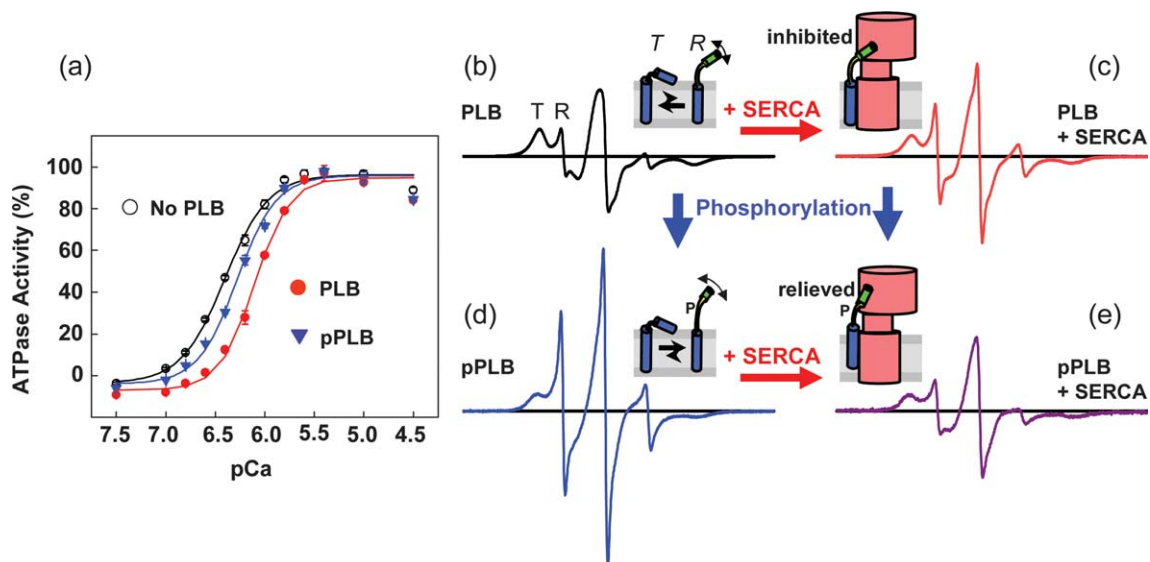


**Figure 3.** Effect of phosphorylation at Ser16 on inhibitory function (a) and EPR-detected dynamics ((b)–(e)) of AFA-PLB, spin-labeled with TOAC at position 11 and reconstituted with SERCA in lipid bilayers. (a) Data sets were fit by equation (1) and plotted as  $V/V_{max}$ . Each point represents the mean ( $n > 6$ ); in most cases, the standard error of the mean (SEM) was smaller than the plotted symbol. (b)–(e) EPR spectra. Top row ((b) and (c)) unphosphorylated. Bottom row ((d) and (e)): phosphorylated. Left column ((b) and (d)): no SERCA. Right column ((c) and (e)): 2 SERCA per PLB. Spectra were normalized to unit concentration by dividing by the double integral. Scan width 120 G at 4 °C. Drawings illustrate a structural model consistent with the data, as discussed in more detail in Figure 7.

This is confirmed in Figure 3(a), which shows that 11-TOAC–AFA-PLB induces a threefold increase in  $K_{Ca}$ , shifting  $pK_{Ca}$  from  $6.40 \pm 0.02$  to  $6.11 \pm 0.02$ . This inhibitory activity was almost completely reversed by synthetically engineered phosphorylation (Figure 3(a)), shifting  $pK_{Ca}$  to  $6.29 \pm 0.02$ . We showed previously that essentially the same inhibitory effects are caused by unlabeled WT-PLB,<sup>25</sup> except that phosphorylation completely reverses the inhibition.<sup>28</sup> These experiments were performed in the presence of excess PLB (10 PLB/SERCA) in order to assess the full effect of spin-labeled PLB, whereas EPR experiments were performed with excess SERCA, in order to assess the full effect of SERCA on PLB. Under EPR conditions (0.5 PLB/SERCA; pCa 6.5) SERCA inhibition was  $42(\pm 10)\%$  of the maximal inhibition (10 PLB/SERCA), indicating that essentially all of the spin-labeled PLB is interacting functionally with SERCA. Under these same EPR conditions, inhibition by spin-labeled PLB was completely relieved at pCa 5, and was relieved by more than half upon PLB phosphorylation, again indicating that the EPR data come from PLB that has normal functional coupling with SERCA.

### Effect of SERCA and phosphorylation on EPR-detected dynamics

As we showed previously,<sup>25</sup> the cytoplasmic domain at position 11 reveals a dynamic equilibrium between two resolved conformations of the peptide backbone, corresponding to ordered (helical, *T* state) and dynamically disordered (extended, *R* state) conformations, as shown in

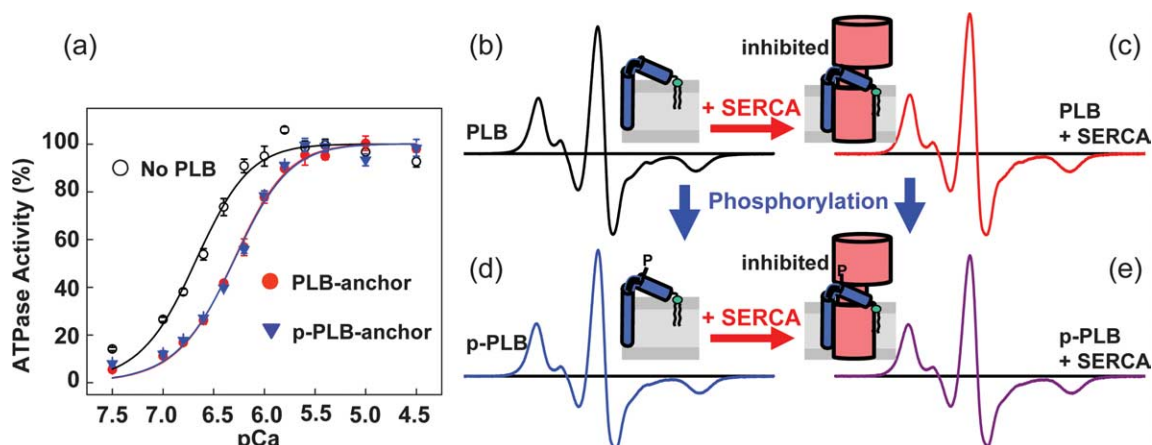


**Figure 4.** Effect of a lipid anchor, attached to the N terminus of 11-TOAC-AFA-PLB, on the data given in Figure 3.

Figure 3(b). Addition of SERCA increases substantially the population in the *R* state (Figure 3(b) to (c)), suggesting that SERCA binds preferentially to this extended state,<sup>27</sup> as depicted in Figure 3(c). Phosphorylation at S16 (Figure 3(b) to (d)) has a qualitatively similar but much greater effect on PLB, increasing substantially the population in the *R* state. On the other hand, SERCA decreases the dynamics (decreases the *R* state population) of phosphorylated PLB (Figure 3(d) to (e)); and phosphorylation decreases the dynamics of SERCA-bound PLB (Figure 3(c) to (e)). If phosphorylation caused PLB to dissociate from SERCA, there would be no difference between spectra (d) and (e) in Figure 3, and phosphorylation of SERCA-bound PLB would increase the *R* state population. Neither is observed; indeed, phosphorylation of SERCA-bound PLB causes the opposite of the predicted effect. Thus phosphorylation, which relieves SERCA inhibition by PLB (Figure 3(a)), does not dissociate PLB from SERCA, but rather changes the conformation of SERCA-bound PLB. As illustrated in Figure 3 and discussed below, these results support a model in which the dynamically disordered (*R*) conformation of the PLB cytoplasmic domain facilitates the binding of PLB to SERCA in an inhibitory complex, but phosphorylation produces an even more disordered PLB conformation that binds differently to SERCA and relieves inhibition.

#### Lipid anchor prevents functional and structural effects of phosphorylation

In the presence of the N-terminal lipid anchor, normal inhibition was observed, but phosphorylation failed to reverse this inhibition (Figure 4(a)) as it does in the absence of the anchor (Figure 3(a)). EPR shows that the ordered *T* conformation of PLB is stabilized by the lipid anchor, and the dynamically disordered *R* conformation is virtually absent, regardless of the presence of SERCA or phosphorylation (Figure 4(b)–(e)). As illustrated in Figure 4 and discussed below, these results support the conclusion that neither the *R* state

nor interaction with the SERCA cytoplasmic domain are required for SERCA inhibition, but both are required for reversal of inhibition due to phosphorylation, as illustrated in Figure 3.

#### Quantitative analysis of dynamics

The results of Figures 3 and 4 are represented more quantitatively in Figure 5, which shows rotational dynamics parameters obtained from spectral simulation and fitting. In the absence of the lipid anchor (Figure 5, left), unphosphorylated PLB (black) spends only 7% of its time in the dynamically disordered *R* state ( $X(R)=0.07$ ), which

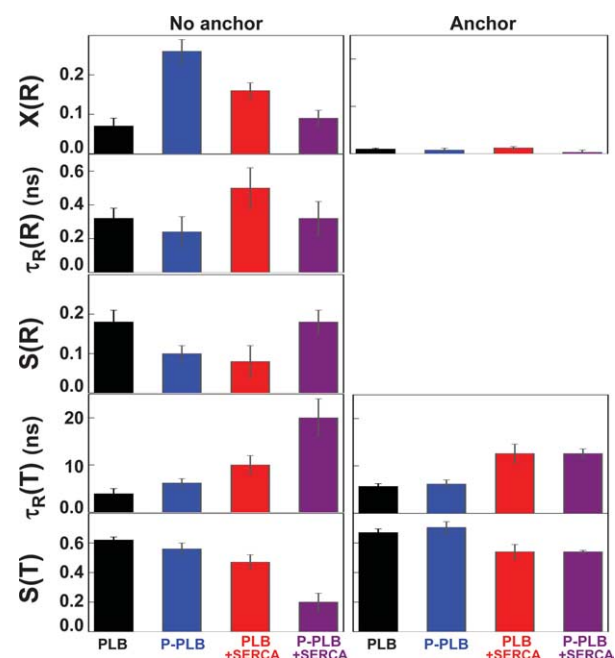


**Figure 5.** Results of EPR spectral analysis of rotational dynamics, for spectra given in Figure 3(b) (left) and Figure 4(b) (right).  $X(R)$  is the mole fraction of the *R* component.  $S$  = order parameter,  $\tau_R$  = rotational correlation time. Parameters  $S(R)$  and  $\tau_R(R)$  were not determined in the presence of the lipid anchor, due to the small values of  $X(R)$ .

is characterized by a subnanosecond correlation time ( $\tau_R=0.3$  ns) and a very low-order parameter ( $S=0.2$ , implying an angular amplitude exceeding  $70^\circ$ ). The predominant  $T$  state is much less dynamic, with a much higher-order parameter ( $S=0.62$ , corresponding to an angular amplitude of about  $40^\circ$ ) and much longer correlation time ( $\tau_R=3$  ns). The primary effect of phosphorylation on isolated PLB (Figure 5, blue) is to increase  $X(R)$  by a factor of 3, while increasing the dynamics of this population (decreasing both  $S$  and  $\tau_R$ ). Thus, phosphorylation increases PLB dynamics in two ways, shifting the equilibrium toward  $R$  and making the  $R$  state even more dynamic, causing it to be hyperextended, as illustrated in Figures 3(b) and 6(b). There was little or no effect of phosphorylation on the mobility of the more restricted  $T$  state (characterized by  $S(T)$  and  $\tau_R(T)$ ), which is stabilized by its contact with the lipid surface.

When unphosphorylated PLB binds to SERCA (Figure 5, red), the  $R$  state becomes more populated and more disordered. Thus, the effect of SERCA is similar to that of phosphorylation, in that it induces an order-to-disorder transition, but the effect is clearly different: SERCA causes a much smaller increase in  $X(R)$ , and it induces much slower dynamics (greater  $\tau_R$ ) for both components. When PLB is phosphorylated in the presence of SERCA (Figure 5, purple), the  $R$  state becomes less populated (decreased  $X$ ) and more ordered (increased  $S$ ), producing dynamics that are quite different from that of phosphorylated PLB in the absence of SERCA (Figure 5, blue). Thus, it is clear that phosphorylation does not relieve inhibition by

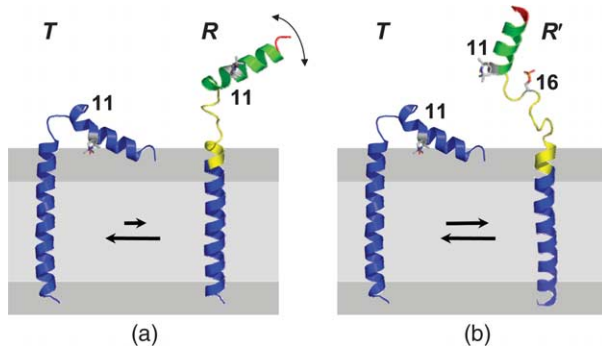


**Figure 6.** Two-state model for PLB conformational dynamics. (a) Unphosphorylated PLB is in equilibrium between ordered ( $T$ ) and dynamically disordered ( $R$ ) conformers. The disordered (extended)  $R$  form binds preferentially to SERCA but does not relieve inhibition. (b) Phosphorylation at Ser16 disorders PLB further, shifting the equilibrium toward the disordered form (right), which itself is more dynamically disordered (hyperextended), and can thus bind to the relief site on SERCA, as depicted by the black spot on SERCA in Figure 3(b). Structures are from solution NMR of unphosphorylated<sup>22</sup> and phosphorylated PLB.<sup>26</sup> The disordered forms (right) are colored spectrally to indicate backbone dynamics, increasing from blue to yellow to green to red.

dissociating PLB from SERCA, but rather decreases the dynamics of bound PLB (Figure 5).

The principal effect of the lipid anchor (Figure 5, right) is to virtually eliminate the dynamic  $R$  state, reducing  $X(R)$  to very low values. The remaining  $T$  state is similar to that observed in the absence of the anchor (Figure 5, right), supporting the conclusion that the  $T$  state is stabilized by contact with the lipid surface. There are slight but significant effects of SERCA on the  $T$  state, increasing  $\tau_R(T)$  but decreasing  $S(T)$ , so it is not clear whether the anchored cytoplasmic domain interacts with SERCA at all. The lipid anchor completely prevents the effects of phosphorylation. These results support the conclusion that phosphorylation acts through its effects on the  $R$  state, which (in the absence of the anchor) increases in population, becomes hyperextended, and interacts with the cytoplasmic domain of SERCA, relieving inhibition (Figure 3).

### **Ca<sup>2+</sup> has no effect on PLB dynamics in the presence of SERCA**

The experiments on SERCA–PLB complexes shown in Figure 3(c) and (e) (no lipid anchor) and in Figure 4(c) and (e) (lipid anchor) were carried out at both  $pCa=6.5$  (where SERCA inhibition is maximal) and  $pCa=5.0$  (where SERCA is not inhibited by PLB), with no difference detected. The EPR spectra at the two  $pCa$  values were essentially identical. Quantitatively, it was found that this variation in  $pCa$  changed the mole fraction  $X(R)$  by no more than 0.01. We cannot rule out the possibility that  $Ca^{2+}$  affects the structure of PLB, or its interactions with SERCA, at a site distant from the spin-labeled site (position 11).<sup>29</sup> However, it is quite clear that (a)  $Ca^{2+}$  does not relieve inhibition by dissociating PLB from SERCA, (b) relief of SERCA inhibition by  $Ca^{2+}$  does not require the PLB cytoplasmic domain to rise above the membrane surface, and (c) phosphorylation and  $Ca^{2+}$  relieve SERCA inhibition through different mechanisms.

## **Discussion**

### **Phosphorylation or SERCA induces an order-to-disorder transition in PLB**

Figure 6 illustrates a model for a two-state conformational equilibrium in PLB, consistent with the data in Figure 3(b) to (d), and with previously published EPR and NMR studies.<sup>22,24,25,27</sup> The cytoplasmic domain of PLB undergoes an equilibrium between at least two states, an ordered state that is similar to the L-shaped NMR solution structure (Figure 6(a),  $T$ ) and a dynamically disordered state in which the central part of this domain is unfolded (Figure 6(a),  $R$ ) and thus able to extend above the membrane surface and interact with the SERCA cytoplasmic domain. Phosphoryl-

ation increases PLB disorder in two ways, shifting the equilibrium toward the *R* state (increasing  $X(R)$ ; Figure 5), and making the *R* state itself even more disordered (decreasing  $S(R)$ ; Figure 5), justifying the new label  $R'$  for this hyperextended state (Figure 6(b)). This phosphorylation-induced order-to-disorder transition is consistent with previous NMR relaxation studies in DPC micelles.<sup>26</sup> Since only the phosphorylated state relieves SERCA inhibition, we propose that the hyperextended  $R'$  state is required to make the proper contact with SERCA to reverse the inhibitory interaction in the transmembrane domain, as illustrated in Figure 6(b).

At first glance, it is surprising that CD data indicate a negligible effect of phosphorylation on helicity ( $-3(\pm 5)\%$ ) for isolated PLB, while both EPR and NMR indicate a substantial decrease in helical order. However, both EPR and NMR indicate that the portion of PLB that takes part in the order-to-disorder transition is small. NMR and EPR data together suggest that the affected region extends approximately from residue 10 to 27.<sup>25,26,30</sup> Of these 18 residues, 13 are helical in the proposed *T* state. Thus, even if we assume that all 13 of these residues shift from helix to coil in the *T* to *R* transition, the predicted change in helicity over the entire PLB would be  $-13/52 = -25\%$ . The EPR observation is that the labeled site increases its fraction disordered by  $19(\pm 5)\%$  upon phosphorylation (Figure 5). If this corresponds to the magnitude of the *R*-to-*T* transition induced by phosphorylation, it predicts a change in helicity by  $-4\%$ , which is well within the range of values consistent with the CD measurement ( $-3(\pm 5)\%$ ).

### A phosphorylation-induced change in structural dynamics of SERCA-bound PLB relieves inhibition

Figure 7 illustrates a model, elaborating on the illustrations in Figures 3 and 6, consistent with the EPR data in the present study and the NMR data in the related paper.<sup>31</sup> PLB is in a dynamic equilibrium between ordered (*T*) and dynamically disordered

(*R*) structural states (Figure 7(a)). SERCA binds preferentially to the *R* state of PLB in both the absence (Figure 7(b)) and presence (Figure 7(d)) of phosphorylation. In the absence of phosphorylation (Figure 7(b)), PLB is not sufficiently extended to reach the relief site on SERCA (depicted as a black target zone on SERCA) so SERCA remains inhibited due to interactions between specific portions of the two transmembrane domains (highlighted in white in Figure 7). In contrast, the hyperextended form of pPLB (Figure 7(c)) does reach the relief site on SERCA, transiently forming the collision complex of Figure 7(d). SERCA binding then reduces the dynamics of phosphorylated PLB (as shown in Figures 3 and 5), resulting in a less extended, more ordered form, which could cause the loss of SERCA inhibition by displacing the inhibitory transmembrane interactions between PLB and SERCA, as illustrated by the separation of white zones in Figure 7(e).

### Lipid anchor prevents reversal of inhibition by blocking formation of disordered state of PLB

The N-terminal lipid stabilizes the ordered *T* state of PLB and prevents the formation of the disordered (extended) *R* state (Figure 4(b)–(e)), but does not prevent inhibition by PLB (Figure 4(a)), showing that inhibition does not require an interaction between the extended form of PLB and the SERCA cytoplasmic domain. However, the anchor does prevent reversal of inhibition due to phosphorylation (Figure 4(a)), probably because it blocks formation of the dynamically disordered (hyperextended)  $R'$  form of the PLB cytoplasmic domain, which reverses SERCA inhibition by contacting a specific relief site on the SERCA cytoplasmic domain (Figure 7). This provides strong support for the importance of the dynamically disordered form of PLB in reversal of SERCA inhibition.

### Relationship to NMR study

This study is closely related to a parallel study in which NMR was used to detect the effects of phosphorylation on the PLB–SERCA interaction.<sup>31</sup> These two studies yield consistent results and are quite complementary to each other. Like the present EPR study, the NMR study observes spectroscopic signals from the peptide backbone of monomeric PLB, and inhibition of SERCA was shown to be relieved by  $\text{Ca}^{2+}$  or phosphorylation under NMR conditions. While the present study is limited to a single labeled site, the NMR study reports information from every residue of PLB. Unlike the present study in lipid membranes, the NMR study was performed in detergent micelles, as required to obtain high-resolution data. While NMR can only observe directly the signal from free (unbound) PLB and the signals are only indirectly related to peptide dynamics, EPR detects both free and bound components with equal sensitivity and reports directly on rotational dynamics of the backbone.

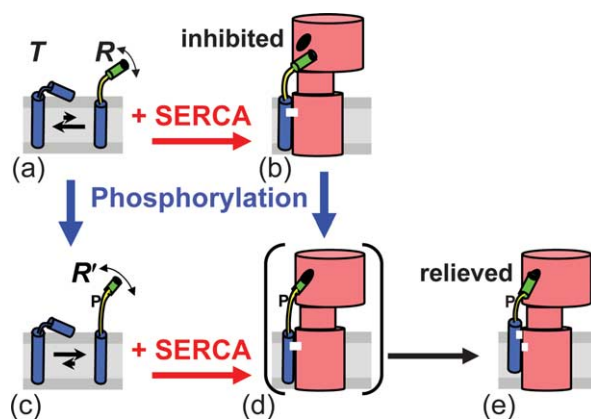


Figure 7. Schematic structural model for the mechanism of SERCA inhibition and relief by PLB.

Taken together, the EPR and NMR results show that a large portion of the cytoplasmic domain of PLB undergoes a disorder-to-order transition upon phosphorylation, and that phosphorylation changes the structural dynamics of PLB without dissociating the two proteins. NMR data also suggest that phosphorylation increases the cooperativity of the SERCA–PLB interaction, supporting a cooperative allosteric model for this regulatory system.

## Conclusion

EPR spectroscopy of a TOAC spin label attached rigidly to the peptide backbone at position 11 in the cytoplasmic domain of PLB shows that PLB phosphorylation at Ser16 induces an order-to-disorder (*T* to *R*) transition in the cytoplasmic domain of PLB, and it is this dynamically disordered (hyperextended) *R* structural state that rises above the membrane surface and binds to the SERCA cytoplasmic domain in a conformation that relieves SERCA inhibition. An N-terminal lipid anchor, which prevents the cytoplasmic domain of PLB from rising above the membrane surface and abolishes the dynamically disordered structural state, inhibits PLB normally but prevents the relief of inhibition by phosphorylation. Micromolar  $[Ca^{2+}]$  reverses PLB-dependent inhibition without a detectable change in cytoplasmic domain dynamics and without the need for the PLB cytoplasmic domain to rise above the membrane surface. Thus, it is clear that neither  $Ca^{2+}$  nor PLB phosphorylation acts by dissociating PLB from SERCA, and that  $Ca^{2+}$  and PLB phosphorylation relieve SERCA inhibition by distinct mechanisms.

## Materials and Methods

### Synthesis of TOAC-labeled PLB

Figure 1 (bottom) shows the sequence of the synthesized monomeric AFA-PLB peptide that incorporates the spin-labeled amino acid TOAC at position 11. The solid-phase synthesis and characterization of this peptide were reported.<sup>21,25,32,33</sup> In order to obtain a derivative of spin-labeled PLB that has its N terminus anchored in the lipid bilayer, dialkyl 1', 3'-dioctadecyl-*N*-succinyl-L-glutamate (lipid tail) was linked to 11-TOAC–AFA-PLB through the N-terminal amino group. The synthesis of novel dialkyl chain amphiphiles containing peptides and its application on PLB was supported previously.<sup>25,34</sup>

Phosphorylation at Ser16 was accomplished either by incorporation as Fmoc-Ser[PO(OBzl)OH] (Novabiochem, San Diego, CA) during peptide synthesis or by cAMP-dependent protein kinase (PKA)<sup>26</sup> after reconstitution,<sup>35</sup> with essentially the same results, both on inhibitory function and on EPR. Phosphorylation by PKA was greater than 80% complete, as determined using anti-PLB antibody (1D11), and the anti-phosphoserine PLB (285) antibody<sup>36</sup> on Western blots.

### Chemical and functional analysis

Mass spectrometry (MALDI-TOF), Edman protein sequencing, amino acid analysis, circular dichroism,<sup>21</sup> inhibitory function,<sup>25</sup> and EPR spectroscopy were used to establish the high purity and functional integrity of the spin-labeled peptides. Each PLB derivative was reconstituted in lipid bilayer membranes (DOPC/DOPE, 4:1) with purified SERCA at molar ratios of 10 PLB/SERCA and 700 lipids/SERCA,<sup>28,35</sup> and the Ca dependence of ATPase activity was measured at 25 °C.<sup>32</sup> The initial ATPase rate  $V$  was measured as a function of pCa (calculated as described<sup>37</sup>), and the data were fit by the Hill equation:

$$V = V_{\max}/[1 + 10^{n(pK_{Ca}-pCa)}] \quad (1)$$

to determine  $V_{\max}$ ,  $pK_{Ca}$  (the pCa value when  $V = V_{\max}/2$ ), and  $n$  (Hill coefficient).  $V_{\max}$  was obtained from the fit, and the data were plotted as  $V/V_{\max}$  versus pCa. The main goal was to determine the shift in  $pK_{Ca}$  caused by PLB.

### EPR spectroscopy

For EPR experiments, TOAC–PLB was reconstituted into lipid vesicles containing DOPC/DOPE (4:1; 200 lipids per PLB) in the presence and absence of excess SERCA.<sup>24</sup> Measurements were conducted in low Ca (pCa 6.5) buffer (50 mM KCl, 5 mM MgCl<sub>2</sub>, 0.5 mM EGTA, 210 μM CaCl<sub>2</sub>, 50 mM Mops (pH 7.0)), where the inhibitory effect of PLB was maximal, and high Ca (pCa 5.0) buffer (same as low Ca, except 489 μM CaCl<sub>2</sub>), where the inhibitory effect of PLB was negligible.<sup>12</sup> The concentration of SERCA was twice that of TOAC–PLB, such that further increase had no effect on EPR spectra. The concentration of TOAC–PLB was determined by amino acid analysis and SERCA concentration by the Lowry method.<sup>38</sup>

EPR spectra (Figures 3 and 4) were acquired using a Bruker EleXsys 500 spectrometer with the SHQ cavity. Samples (20 μl in a 0.6 mm i.d. quartz capillary) were maintained at 4 °C using the Bruker temperature controller with a quartz Dewar insert. The field modulation frequency was 100 kHz, with a peak-to-peak amplitude of 1 G. The microwave power was 12.6 mW, producing moderate saturation (so that signal intensity was at least 50% of maximum) without significant effect on the spectral lineshape.

EPR spectra were calculated as a sum of one or two components, each component produced by a population having a static isotropic distribution of membrane orientations and undergoing rotational diffusion in a restricting potential (defined by order parameter  $S$ ) with a single rotational correlation time ( $\tau_R$ ). Components were simulated with NLSL<sup>39</sup> on an IBM SP; the MOMD model was used, and the NLSL parameters  $\bar{R}$  (diffusion rate) and  $c_{20}$  (first ordering potential parameter) were set to produce the desired  $\tau_R$  and  $S$ . Magnetic tensors were determined from spectra obtained at –60 °C. Lorentzian linewidths of 1 G and 2 G were used for narrow and broad spectral components, respectively. Experimental spectra were fit by summing simulated components. Error estimates for  $\tau_R$  and  $S$  (Figure 5) were determined from the range of input values of these parameters for which the spectral splittings and linewidths were within experimental uncertainty of observed values. Angular amplitudes of motion were estimated from the expression  $\theta_c = \cos^{-1}[0.5(1 + 8S)^{1/2} - 0.5]$ , where  $\theta_c$  is the radius of the cone that limits the motion.

## Acknowledgements

This work was supported by grants to D.D.T. (NIH GM27906) and C.B.K. (AHA 9930083N). Supercomputer time was provided by the Minnesota Supercomputing Institute. We thank Razvan Cornea, Gianluigi Veglia and Nathaniel Traaseth for insightful discussions; Deborah Winters for assistance in molecular modeling and graphics; Yuri Nesmelov for assistance with EPR spectroscopy; Florentin Nitu for technical assistance; Nathan Lockwood for providing the lipid anchor; Thomas Krick for assistance with mass spectrometry; Jinny Johnson and Lawrence Dangott (Protein Chemistry Laboratory, Texas A&M University) for amino acid analysis.

## References

- Lindemann, J. P., Jones, L. R., Hathaway, D. R., Henry, B. G. & Watanabe, A. M. (1983). Beta-adrenergic stimulation of phospholamban phosphorylation and Ca<sup>2+</sup>-ATPase activity in guinea pig ventricles. *J. Biol. Chem.* **258**, 464–471.
- MacLennan, D. H. & Kranias, E. G. (2003). Phospholamban: a crucial regulator of cardiac contractility. *Nature Rev. Mol. Cell Biol.* **4**, 566–5877.
- Haghighi, K., Kolokathis, F., Pater, L., Lynch, R. A., Asahi, M., Gramolini, A. O. *et al.* (2003). Human phospholamban null results in lethal dilated cardiomyopathy revealing a critical difference between mouse and human. *J. Clin. Invest.* **111**, 869–876.
- Minamisawa, S., Sato, Y., Tatsuguchi, Y., Fujino, T., Imamura, S., Uetsuka, Y. *et al.* (2003). Mutation of the phospholamban promoter associated with hypertrophic cardiomyopathy. *Biochem. Biophys. Res. Commun.* **304**, 1–4.
- Sande, J. B., Sjaastad, I., Hoen, I. B., Bokenes, J., Tonnessen, T., Holt, E. *et al.* (2002). Reduced level of serine(16) phosphorylated phospholamban in the failing rat myocardium: a major contributor to reduced SERCA2 activity. *Cardiovasc. Res.* **53**, 382–391.
- Schmidt, A. G., Edes, I. & Kranias, E. G. (2001). Phospholamban: a promising therapeutic target in heart failure? *Cardiovasc. Drugs Ther.* **15**, 387–396.
- Minamisawa, S., Hoshijima, M., Chu, G., Ward, C. A., Frank, K., Gu, Y. *et al.* (1999). Chronic phospholamban-sarcoplasmic reticulum calcium ATPase interaction is the critical calcium cycling defect in dilated cardiomyopathy. *Cell*, **99**, 313–322.
- Thomas, D. D., Reddy, L. G., Karim, C. B., Li, M., Cornea, R., Autry, J. M. *et al.* (1998). Direct spectroscopic detection of molecular dynamics and interactions of the calcium pump and phospholamban. *Ann. N Y Acad. Sci.* **853**, 186–194.
- MacLennan, D. H., Kimura, Y. & Toyofuku, T. (1998). Sites of regulatory interaction between calcium ATPases and phospholamban. *Ann. N Y Acad. Sci.* **853**, 31–42.
- Kimura, Y., Kurzydowski, K., Tada, M. & MacLennan, D. H. (1997). Phospholamban inhibitory function is activated by depolymerization. *J. Biol. Chem.* **272**, 15061–15064.
- Cornea, R. L., Jones, L. R., Autry, J. M. & Thomas, D. D. (1997). Mutation and phosphorylation change the oligomeric structure of phospholamban in lipid bilayers. *Biochemistry*, **36**, 2960–2967.
- Mueller, B., Karim, C. B., Negrashov, I. V., Kutchai, H. & Thomas, D. D. (2004). Direct detection of phospholamban and sarcoplasmic reticulum Ca-ATPase interaction in membranes using fluorescence resonance energy transfer. *Biochemistry*, **43**, 8754–8765.
- Mueller, B., Zhao, M., Negrashov, I. V., Bennett, R. & Thomas, D. D. (2004). SERCA structural dynamics induced by ATP and calcium. *Biochemistry*, **43**, 12846–12854.
- Negash, S., Yao, Q., Sun, H., Li, J., Bigelow, D. J. & Squier, T. C. (2000). Phospholamban remains associated with the Ca<sup>2+</sup>- and Mg<sup>2+</sup>-dependent ATPase following phosphorylation by cAMP-dependent protein kinase. *Biochem. J.* **351**, 195–205.
- Chen, B. & Bigelow, D. J. (2002). Phosphorylation induces a conformational transition near the lipid-water interface of phospholamban reconstituted with the Ca-ATPase. *Biochemistry*, **41**, 13965–13972.
- Li, J., Bigelow, D. J. & Squier, T. C. (2004). Conformational changes within the cytosolic portion of phospholamban upon release of Ca-ATPase inhibition. *Biochemistry*, **43**, 3870–3879.
- Li, J., Xiong, Y., Bigelow, D. J. & Squier, T. C. (2004). Phospholamban binds in a compact and ordered conformation to the Ca-ATPase. *Biochemistry*, **43**, 455–463.
- Reddy, L. G., Jones, L. R. & Thomas, D. D. (1999). Depolymerization of phospholamban in the presence of calcium pump: a fluorescence energy transfer study. *Biochemistry*, **38**, 3954–3962.
- Li, M., Reddy, L. G., Bennett, R., Silva, N. D., Jr, Jones, L. R. & Thomas, D. D. (1999). A fluorescence energy transfer method for analyzing protein oligomeric structure: application to phospholamban. *Biophys. J.* **76**, 2587–2599.
- Autry, J. M. & Jones, L. R. (1997). Functional Co-expression of the canine cardiac Ca<sup>2+</sup> pump and phospholamban in *Spodoptera frugiperda* (Sf21) cells reveals new insights on ATPase regulation. *J. Biol. Chem.* **272**, 15872–15880.
- Lockwood, N. A., Tu, R. S., Zhang, Z., Tirrell, M. V., Thomas, D. D. & Karim, C. B. (2003). Structure and function of integral membrane protein domains resolved by peptide-amphiphiles: application to phospholamban. *Biopolymers*, **69**, 283–292.
- Zamoon, J., Mascioni, A., Thomas, D. D. & Veglia, G. (2003). NMR solution structure and topological orientation of monomeric phospholamban in dodecylphosphocholine micelles. *Biophys. J.* **85**, 2589–2598.
- Mascioni, A., Karim, C., Zamoon, J., Thomas, D. D. & Veglia, G. (2002). Solid-state NMR and rigid body molecular dynamics to determine domain orientations of monomeric phospholamban. *J. Am. Chem. Soc.* **124**, 9392–9393.
- Kirby, T. L., Karim, C. B. & Thomas, D. D. (2004). Electron paramagnetic resonance reveals a large-scale conformational change in the cytoplasmic domain of phospholamban upon binding to the sarcoplasmic reticulum Ca-ATPase. *Biochemistry*, **43**, 5842–5852.
- Karim, C. B., Kirby, T. L., Zhang, Z., Nesmelov, Y. & Thomas, D. D. (2004). Phospholamban structural dynamics in lipid bilayers probed by a spin label rigidly coupled to the peptide backbone. *Proc. Natl Acad. Sci. USA*, **101**, 14437–14442.
- Metcalfe, E. E., Traaseth, N. J. & Veglia, G. (2005). Serine 16 phosphorylation induces an order-to-disorder transition in monomeric phospholamban. *Biochemistry*, **44**, 4386–4396.

27. Zamoon, J., Nitu, F., Karim, C., Thomas, D. D. & Veglia, G. (2005). Mapping the interaction surface of a membrane protein: unveiling the conformational switch of phospholamban in calcium pump regulation. *Proc. Natl Acad. Sci. USA*, **102**, 4747–4752.
28. Reddy, L. G., Autry, J. M., Jones, L. R. & Thomas, D. D. (1999). Co-reconstitution of phospholamban mutants with the Ca-ATPase reveals dependence of inhibitory function on phospholamban structure. *J. Biol. Chem.* **274**, 7649–7655.
29. Jones, L. R., Cornea, R. L. & Chen, Z. (2002). Close proximity between residue 30 of phospholamban and cysteine 318 of the cardiac Ca<sup>2+</sup> pump revealed by intermolecular thiol cross-linking. *J. Biol. Chem.* **277**, 28319–28329.
30. Metcalfe, E., Zamoon, J., Thomas, D. D. & Veglia, G. (2004). (1)H/(15)N heteronuclear NMR spectroscopy shows four dynamic domains for phospholamban reconstituted in dodecylphosphocholine micelles. *Biophys. J.* **87**, 1205–1214.
31. Traaseth, N. J., Thomas, D. D. & Veglia, G. (2006). Effects of Ser16 phosphorylation on the allosteric transitions of phospholamban/Ca<sup>2+</sup>-ATPase complex. *J. Mol. Biol.* In the press.
32. Karim, C. B., Paterlini, M. G., Reddy, L. G., Hunter, G. W., Barany, G. & Thomas, D. D. (2001). Role of cysteine residues in structural stability and function of a transmembrane helix bundle. *J. Biol. Chem.* **276**, 38814–38819.
33. Karim, C. B., Marquardt, C. G., Stamm, J. D., Barany, G. & Thomas, D. D. (2000). Synthetic null-cysteine phospholamban analogue and the corresponding transmembrane domain inhibit the Ca-ATPase. *Biochemistry*, **39**, 10892–10897.
34. Berndt, P., Fields, G. B. & Tirrell, M. (1995). Synthetic lipidation of peptides and amino acids: monolayer structure and properties. *J. Am. Chem. Soc.* **117**, 9515–9522.
35. Reddy, L. G., Cornea, R. L., Winters, D. L., McKenna, E. & Thomas, D. D. (2003). Defining the molecular components of calcium transport regulation in a reconstituted membrane system. *Biochemistry*, **42**, 4585–4592.
36. Mayer, E. J., Huckle, W., Johnson, R. G., Jr & McKenna, E. (2000). Characterization and quantitation of phospholamban and its phosphorylation state using antibodies. *Biochem. Biophys. Res Commun.* **267**, 40–48.
37. Fabiato, A. & Fabiato, F. (1979). Calculator programs for computing the composition of the solutions containing multiple metals and ligands used for experiments in skinned muscle cells. *J. Physiol. (Paris)*, **75**, 463–505.
38. Lowry, O. H., Rosebrough, N. J., Farr, A. L. & Randall, R. J. (1951). Protein measurement with the Folin phenol reagent. *J. Biol. Chem.* **193**, 265–275.
39. Budil, D. E., Lee, S., Saxena, S. & Freed, J. H. (1996). Non-linear-least-squares analysis of slow-motion EPR spectra in one and two dimensions using a modified Levenberg–Marquardt algorithm. *J. Magn. Reson. A*, **120**, 155–189.

*Edited by M. F. Summers*

(Received 8 December 2005; received in revised form 3 February 2006; accepted 16 February 2006)  
Available online 9 March 2006